Validation of Spectral Simulation Tools for the Prediction of Indoor Daylight Exposure

Clotilde Pierson[1,2], Mariëlle Aarts[2], Marilyne Andersen[1]
[1]École Polytechnique Fédérale de Lausanne (EPFL), Lausanne, Switzerland
[2]Eindhoven University of Technology (TU/e), Eindhoven, The Netherlands

Abstract

A growing area of research focuses on the relationship between ocular light exposure and the non-visual responses. In order to accelerate research on this topic and improve building design, reliable spectral simulation tools are needed. This study aims at validating two of them, *Lark* and *ALFA*, by comparing their outcomes against daylight measurements. The goal is to assess how reliable these tools are in predicting spectral irradiance under different skies for indoor spaces. While spectral irradiance can in principle be simulated with a similar accuracy as for photopic values, there are some caveats in the current versions of both platforms.

Key Innovations

- Use of spectral simulation tools for indoor daylit scenes
- Validation of existing simulation tools in terms of absolute spectral irradiance
- Comparison between spectral and RGB simulations

Practical Implications

Once fully validated, spectral simulation tools like *Lark* or *ALFA* can provide a powerful support for decision-making regarding light exposure when it comes to meeting physiological needs in indoor environments.

Introduction

Since the discovery of a new photoreceptor in the eye – the intrinsically photosensitive retinal ganglion cells (ipRGC) containing the photopigment melanopsin (Brainard et al., 2001) –, a growing area of research has been focusing on the relationship between ocular light exposure and the so-called non-visual responses to light. These non-visual responses to light have been shown to impact our alertness, sleep cycles, mood, and other neurobehavioral processes (Xiao et al., 2021), which raises awareness on the importance of a proper light exposure for our health and well-being. Considering that we spend the vast majority of our time indoors, it becomes urgent to identify what a proper light exposure means in the built environment, and to anticipate design decisions that could negatively affect our access to daylight. As we gain a deeper understanding of the mechanisms behind non-visual effects of light through laboratory and field studies, more and more refined models are starting to emerge. Many of them aim to link ocular light exposure with neurophysiological responses, which requires to evaluate what characterizes the light reaching the eye: its intensity, timing, pattern, etc., and its spectral content. This last characteristic calls for spectrally resolved simulation workflows, or simply "spectral simulations" i.e., simulations in which light transport computations, material and light parameters span the entire visible spectrum and are defined based on N channels with N being more than three (Inanici et al., 2015).

According to this definition, most light simulation platforms (Ayoub, 2020; Ochoa et al., 2012) – including the ubiquitous *Radiance* rendering engine (Ward, 1987), are not proper spectral simulation tools, since they are usually based on a three-dimensional (e.g., RGB) color space, though they have already been used to discuss non-visual responses to light (Acosta et al., 2017; Amirazar et al., 2018; Amundadottir et al., 2017; Amundadottir et al., 2013; Andersen et al., 2011; Borisuit et al., 2016; Konis, 2016; Pechacek et al., 2008). A framework based on α-opic spectral sensitivity functions (Lucas et al., 2014) has since been adopted by the International Commission on Illumination (CIE) to describe the ability of optical radiation to trigger non-visual effects of light in humans (CIE, 2018). What the underlying simulation workflows have in common, however, is that they rely on the post-processing of computed *photopic* light values (based on the standardized $V(\lambda)$ curve) to derive an output indicative of the non-visual potential of the simulated light (usually based on the action spectrum of the melanopsin photopigment (Brainard et al., 2001)) and are based on non-spectral material definitions and sky models.

To address this limitation, spectral simulation workflows were developed (Geisler-Moroder & Dür, 2010; Wandachowicz, 2006), but as these workflows required deep knowledge in *Radiance* and strong coding skills to be implemented, a new spectral simulation tool called *Lark* was released (Inanici et al., 2015). Borrowing from the N-step method (Yang & Maloney, 2001) initially used for applications in psychophysics (Delahunt & Brainard, 2004; Ruppertsberg & Bloj, 2006, 2008), it relies on the physically accurate *Radiance* rendering engine to offer a "spectral" resolution through the following three steps:

1. dividing the spectrum of the simulated light source(s) into N (a multiple of 3) consecutive wavebands,
2. running a standard RGB simulation for each triplet of consecutive wavebands, and
3. combining the outputs of the multiple RGB simulation calls with some postprocessing.

Lark performs simulations in 9 color channels and allows the users to design and analyze daylight with a "spectral" resolution while considering local skies, exterior context, glazing optics, surface materials, interior design, and viewer location. It has a relatively user-friendly interface and is a free and open-source tool (Inanici & ZGF Architects LLP, 2015) which runs on the *Grasshopper* plugin in *Rhinoceros 3D* (McNeel et al., 2020).

Another user-friendly spectral simulation tool, *ALFA* (Adaptive Lighting for Alertness), is a licensed tool that was recently released (Solemma LLC & Alertness CRC, 2018). *ALFA* runs directly as a plugin to *Rhinoceros 3D* and can conduct physically accurate simulations in 81 color channels thanks to the program spectree. Basically, the method applied in *ALFA* consists of inserting a spectrum at the light source in the simulated scene and using *Radiance*'s backward raytracing approach to move back toward the sensor location, accounting for spectral reflectance and transmittance at each material interaction. While the spectra resulting from this method are similar to those resulting from a spectral simulation using the N-step approach, the method requires much less computing overhead than repeating 27 times a standard RGB simulation. The respective characteristics of both tools can be compared in Table 1.

Table 1: Simulation features for ALFA and Lark.

Features	*ALFA*	*Lark*
Nb channels	81	9
Geometry	Rhinoceros 3D model	Rhinoceros 3D model
Materials	spectrally defined (material library or property inputs)	spectrally defined (material property inputs)
Simulated sky	spectrally defined (existing atmospheric profiles)	"spectrally" defined (global sky SPD and irradiance)
Simulated sun	spectrally defined	non-spectrally defined (white source)
Availability	licensed	open-source

So far, only one study has compared *Lark*, *ALFA*, and standard RGB simulations for their visual, spectral and colorimetric accuracy (Balakrishnan & Jakubiec, 2019). In this study, visual aspects of the rendered images (including their simulated color coordinates) and their associated (simulated) spectral power distributions (SPD) were evaluated against the corresponding measured data for complex outdoor urban scenes under daylight. The results of the study showed that, due to the difference in the way the sun and sky are modeled in the three tools, *Lark* produces the closest color coordinates and the most accurate SPD for uniform skies (i.e., overcast) compared to measurements, whereas *ALFA* performs best for clear skies. However, to this date, no study has looked at validating *ALFA* or *Lark* in terms of absolute spectral irradiance. With the fast-growing interest for design applications related to the non-visual responses to light, the validation of these spectral simulation tools is becoming urgent to ensure the reliability of their outcomes to inform design decisions (Altenberg Vaz & Inanici, 2020; Potočnik & Košir, 2021). The aim of this study is to validate *ALFA* and *Lark* under real daylight conditions experienced indoors.

Methods

The validation of a simulation tool requires to determine the degree to which the tool allows us to offer an accurate representation of the real world. The methodology applied here consists in comparing spectral irradiance under daylight conditions at three desk positions measured for a certain period of time in an office-like laboratory module against the corresponding spectral simulation outcomes.

Measurements

For this study, two types of measurements are required: those used to build the validation dataset (measurements of real-world spectral irradiance), and those used to run the simulations. For the validation dataset, time series of spectral irradiance measured at eye level in seating position (i.e., 1.2 m above the floor) were collected. The measurements of spectral irradiance were taken every 6 minutes between 8am and 6pm over several days. A first series of measurements was collected between January 30 and March 17, 2020, in a west-oriented office-like module in Eindhoven (51.45°N – 5.48°E). As the data collected contained very few clear sky conditions, it was decided to collect a second series of measurements in a similar but south-oriented office-like module in Lausanne (46.52°N – 6.56°E) between August 21 and September 1, 2020.

In both locations, spectral irradiance was measured simultaneously for three desk positions. The desks were set up as in Figure 1 to generate three distinct lighting conditions. Spectral irradiance was measured by Ocean Insight spectrometers – the USB4000 model in Eindhoven and the Jaz model in Lausanne – that had all been previously calibrated with a radiometric calibrated light source. Hagner luxmeters were located next to the spectrometers (except for desk 3 in Lausanne) and simultaneously measured vertical illuminance. Collected illuminance values were used to check the validity of the simulation model and scale the measured spectral irradiance if needed. Additionally, NanoLambda NSP32 spectrometers measured the spectral irradiance for the desks in Lausanne. Two desks in Eindhoven were also equipped with a Bee-Eye, i.e., a luminance distribution measurement device (Kruisselbrink et al., 2017).

Measurements were also needed to simulate spectral irradiance at the three desks. To create a 3D model for the two test modules in *Rhinoceros 3D*, their actual dimensions and furniture (i.e., desks and computer screens) were accounted for. The buildings and trees surrounding the laboratory cells were also modeled based on *OpenStreetMap* data (OpenStreetMap contributors, 2017). A ground was added in both 3D models, as it appeared that the default ground in *Lark* is defined as red. Regarding materials, their spectral reflectance was measured with a Konica Minolta CM-2600d and CM-700d spectrophotometer in Eindhoven and Lausanne respectively and used as inputs for the spectral simulations performed. As the spectral transmittance of the glazing could not be measured for practical reasons, it was evaluated by the Optics software (LBNL, 2013) then reduced by 8% in Eindhoven to account for atmospheric pollutants (Tregenza et al., 1999). No reduction was applied for Lausanne as the windows had just been cleaned. A spectrally constant albedo of 0.2 (Gul et al., 2018) and reflectance of 0.35 were used for the ground and the surrounding buildings respectively in both models. The trees were modeled as translucent objects (constant spectrum, no reflection and scattering), based on the transparencies of tree crowns (Helliwell, 2012) in winter for Eindhoven (i.e., bare branch) and in summer for Lausanne (i.e., full leaf).

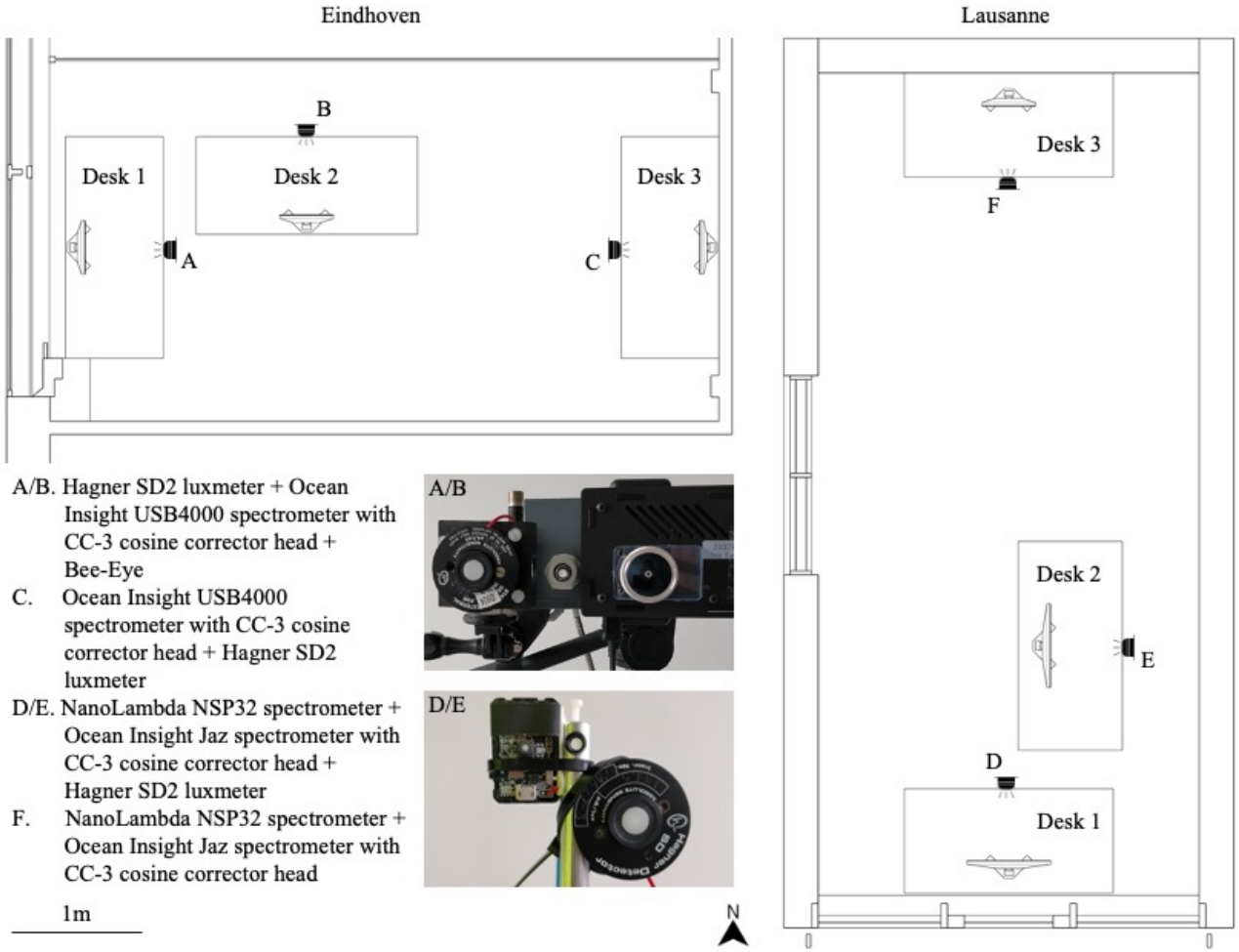

Figure 1: Experimental set up in the two office-like laboratory modules; all sensors face the computer screen at eye level.

To generate the spectral sky model corresponding to each data point in the validation dataset, different measurements are required as inputs to *ALFA* and *Lark* besides the location and time. In *ALFA*, the spectral sky model is generated based on a spectral sun and sky that are precomputed in a radiative transfer library, called libRadtran, that uses measured atmospheric profiles. Therefore, the only additional input required is the sky condition, which can be set as clear, hazy, overcast or heavy rain clouds. In order to classify the multiple skies that occurred during the measurement campaign into these four categories, the diffuse horizontal (DHI) and direct normal (DNI) irradiance were measured simultaneously to the measurements of spectral irradiance at the desks, with an EKO MS-802 pyranometer and an EKO MS-56 pyrheliometer located on the roof of the building for the Eindhoven model and with a Delta-T SPN1 pyranometer located on the roof of a neighboring building for the Lausanne model. As recommended in a validation study of the SPN1 pyranometer (Badosa et al., 2014), the DHI and DNI measured values were multiplied respectively by 1.05 and 0.95 to account for the slight inaccuracies of the device. Based on these two variables and the solar zenith angle, the sky's clearness coefficient ε was calculated and used to classify the sky between clear ($\varepsilon >= 4.5$), intermediate/hazy ($1.065 < \varepsilon < 4.5$), and overcast ($\varepsilon <= 1.065$) skies (Perez et al., 1990). In situ pictures of the skies and precipitation data from local weather stations were also collected to subdivide the skies in the overcast category between the heavy rain clouds and overcast categories of *ALFA*.

In *Lark*, the spectral sky model is generated based on a spectral sky and a non-spectral, equal-energy white sun. Therefore, the spectral power distribution (SPD) of the sky is required as an input in *Lark*. The SPD was measured with an Ocean Insight USB4000 spectrometer in Eindhoven and an Ocean Insight Flame VIS-NIR spectrometer in Lausanne, protected by a shading ring and located on the roof of the building. As the sky luminance distribution is by default defined in *Lark* through the gensky program (that relies on the CIE standard sky distributions), the script of *Lark* was edited to run the gendaylit program instead, which relies on the Perez sky distributions and offers a luminous efficacy model, as recommended in the literature (Balakrishnan & Jakubiec, 2019). The inputs required for the gendaylit program are the time, the location, the DHI and DNI that were measured as described above, and the dew point temperature, which was measured with a Lufft WS 600 weather station located on the roof of the building for the Eindhoven model, and derived from the relative humidity and air temperature measured by a local weather station from the Federal Office of Meteorology and Climatology in Switzerland for the Lausanne model.

Simulations

Time series of spectral irradiance simulated at eye-level for a seated person are required to complement the time series of measured spectral irradiance for the three desks in both modules so as to make the comparison. Those time series of spectral irradiance were simulated with both *Lark* and *ALFA*. Temporary technical issues prevented data collection for a few days in Eindhoven, resulting in missing input data for some of the *Lark* simulations. The dataset containing the corresponding measured and simulated spectral irradiance is thus larger for *ALFA* than *Lark* since more time steps could be simulated in *ALFA*. In total, the *ALFA* and *Lark* datasets contain respectively 11361 and 8957 data points for the two locations and all three desk positions, for multiple sky conditions (table 2).

Table 2: Composition of the datasets containing the measured and simulated spectral irradiance.

Dataset	*ALFA*	*Lark*
All (N)	11361	8957
Eindhoven | Lausanne (%)	70 | 30	62 | 38
Desk 1 | Desk 2 | Desk 3 (%)	30 | 33 | 37	31 | 34 | 35
Clear | Hazy | Ovc. | Rain (%)	17 | 32 | 32 | 19	13 | 34 | 32 | 21

Before running the spectral simulations in *Lark* and *ALFA*, a basic *Radiance* RGB simulation was run for each time step to validate the simulation models of Eindhoven and Lausanne. The simulations were run on Windows 10 virtual machines with *Rhinoceros 3D* v.6 SR26, *Radiance* v.5.3., *Grasshopper* v.1.0.0007, *Honeybee* v.0.0.65, and *Ladybug* version 0.0.69. The *Radiance* parameters used for the simulations are provided in Table 3.

Table 3: Radiance parameters used for the simulations.

***Radiance* Parameter**	**Setting**
Ambient bounces (-ab)	6
Ambient divisions (-ad)	1000000
Ambient accuracy (-aa)	0
Ambient super-samples (-as)	0
Limit reflections (-lr)	0
Limit weight (-lw)	0.00001

The relative error between measured and simulated vertical illuminances, expressed through Equation (1), was computed for each data point. The distribution of the relative error is plotted by desk for both locations and for each sky type in Figure 2. It should be noted that there were no vertical illuminance measurements available for desk 3 in Lausanne; hence the relative error is only computed for the two other desks.

$$RE\ [\%] = \frac{E_{v,RGB\ simulated} - E_{v,measured}}{E_{v,measured}} * 100 \qquad (1)$$

In the literature, it has been shown that the distribution of relative errors in illuminance between *Radiance* RGB simulations and measurements under daylit indoor conditions is fairly symmetric at the 0% line, and the main body of the distribution is contained within the ±17.5% range (Mardaljevic, 1999). The results obtained for the *Radiance* RGB simulations here present the same characteristics, as can be seen in Figure 2, despite a slightly larger spread. This larger spread might be due to the less accurate sky model used in these simulations compared to the sky models derived from sky-scanning measurements used in Mardaljevic's study. A comparison between the simulated and captured views at desk 1 in Lausanne is provided in Figure 3, although the picture captured at desk 1 was taken after the measurement period in winter, hence the bare branches. Overall, the results of these simulations demonstrate that both models are valid, and the spectral simulations can be run in *ALFA* and *Lark*.

The simulation process for all the time steps was automated in both *Lark* and *ALFA*. First, the constant inputs, such as the materials' spectral reflectance and the locations of the building, were provided to each tool in the required format. Then, both simulation tools were set up in such a way that they loop through all the time steps and that the simulations are automatically run one after the other for the three desks. Since *Lark* runs on the *Grasshopper* plugin, the automation for *Lark* was implemented through the component Fly. The simulations were run on Windows 10 virtual machines, with *Rhinoceros 3D* v.6 SR26, *Grasshopper* v.1.0.0007, *Honeybee* v.0.0.65, *Ladybug* v.0.0.69, *Lark* version 0.0.1, and *Radiance* version 5.3. The *Radiance* parameters used for the simulation in *Lark* are detailed in Table 3. Instead of the default outputs, the RGB values at each desk resulting from each simulation run in *Lark* were extracted. To derive the average spectral irradiance over the waveband corresponding to each RGB value, Equation (2) was applied, in which SI_i is the average spectral irradiance over the waveband i; R_i is the RGB value simulated by *Lark* for the waveband i; 179 is the luminous efficacy in *Radiance*; 683 is the luminous efficacy for monochromatic radiation at the wavelength 555 nm; 107 is the integrated photopic spectral luminous efficiency function. The consecutive wavebands defined in *Lark* have already been published (Inanici et al., 2015).

$$SI_i[W/m^2/nm] = R_i * \frac{179}{683*107} \qquad (2)$$

ALFA, however, does not yet allow any automation in its interface. Therefore, a robotic process automation was used: a *Python* script leveraging the *PyAutoGUI* package controlled the mouse and keyboard to automate the interactions with *ALFA*. The simulations were run on Windows 10 computers, with *Rhinoceros 3D* v.6 SR26, *ALFA* v.0.5.6.99, *Python* v.3.8, and *PyAutoGUI* v.0.9.52. Despite the fact that *ALFA* is based on *Radiance*, only two parameters can be modified through the interface: the ambient bounces (-ab) and the limit weight (-lw), which were respectively set at 6 and 1e-20 (Eindhoven)/1e-25 (Lausanne). The number of passes in *ALFA* was set up at 75 in both models. *ALFA* outputs include the average spectral irradiance over each 5 nm consecutive waveband.

Analyses

The measured and simulated spectral irradiance were then compared through error metrics. Since each data point contains multiple values, i.e., all the spectral irradiance values composing the spectrum over the visible range (380-740nm), the error between the spectra at each desk for each time step was evaluated through the normalized root mean square error (NRMSE) (3) and the median relative bias error (MRBE) (4). These two error metrics were chosen for the distinct information that they provide:

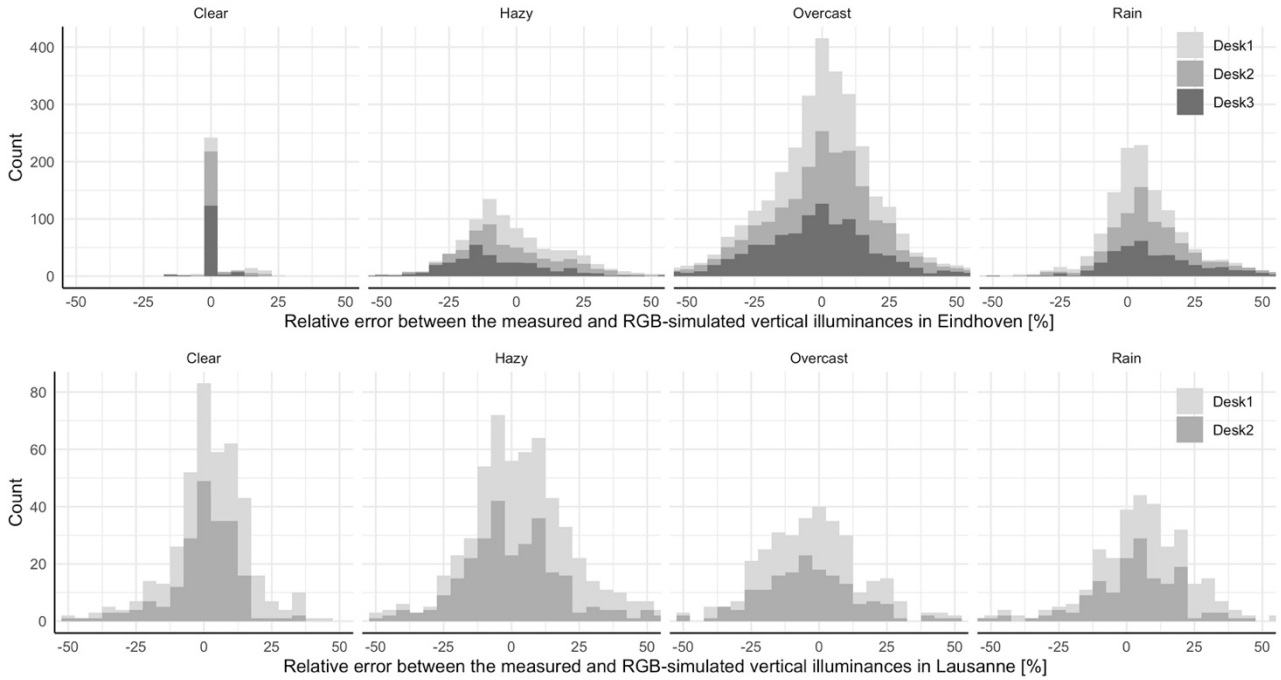

Figure 2: Distribution of RE between the measured and simulated vertical illuminance at eye level by sky condition for both locations and for each desk position.

while the MRBE indicates the tendency of the simulated spectrum to be larger or smaller than the measured one (i.e., the bias), the NRMSE indicates how far the simulated spectrum fluctuates around the measured one (Reinhart & Andersen, 2006).

$$NRMSE\ [-] = \frac{\sqrt{\text{mean}[(SI_{sim,i} - SI_{meas,i})^2]}}{\text{mean}[SI_{meas,i}]} \quad (3)$$

$$MRBE\ [\%] = \text{median}\left[\frac{SI_{sim,i} - SI_{meas,i}}{SI_{meas,i}} * 100\right] \quad (4)$$

In these equations, $SI_{sim,i}$ is the simulated spectral irradiance at the wavelength i; $SI_{meas,i}$ is the measured spectral irradiance at the wavelength i. To summarize the values of these metrics over the entire dataset, the median of the MRBE and the NRMSE were computed.

Results and Discussion

The first performed analysis was the comparison of the simulation error between standard simulations in *ALFA* and in *Lark* (Figure 4). It appears that for such simulations, the *ALFA* simulated spectra tend to have a negative bias and quite a large average fluctuation (median NRMSE ≈ 0.5) around the measured spectra, whereas the *Lark* simulated spectra tend to have no bias and a reasonable fluctuation (median NRMSE < 0.2). Since, by default, the inputs required for simulations in *Lark* are more complete than in *ALFA*, this explains the different errors between the two tools: for a standard simulation in *ALFA*, only the sky type, location, and time have to be defined, while a standard simulation in *Lark* also requires the sky irradiance and SPD.

Figure 3: Captured and simulated view at desk 1 in Lausanne in beginning of afternoon with an intermediate sky.

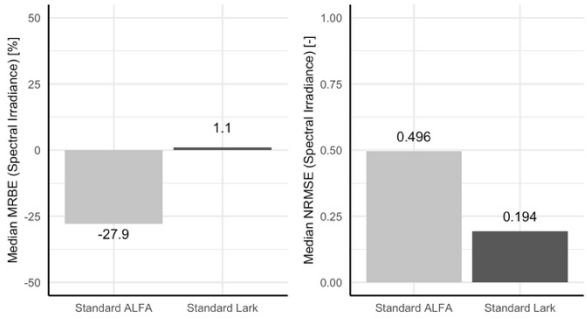

Figure 4: Median MRBE and NRMSE comparison between standard ALFA and Lark simulations.

In view of these results, an unreleased version of *ALFA* was provided to us by the developers, in which the irradiance of the sky model could be scaled based on the measured global sky horizontal irradiance (GHI). A second comparison was performed between simulations in *ALFA* applying the custom scaling of the sky model, and standard simulations in *Lark*, in which this scaling is done by default (Figure 5).

Although the negative bias disappears (or even becomes positive) for *ALFA* simulations when the sky model is scaled with the measured GHI, the average fluctuation from the measured spectra is still large. This is a behavior of *ALFA* that was also observed manually: when the exact same simulation run (same 3D model, same parameters, same computer) is conducted several successive times in

ALFA, a deviation of up to 37% in illuminance was observed in the results. The developers of *ALFA* are aware of this issue and are currently working on solving it. It was therefore decided to focus on the simulations with *Lark*.

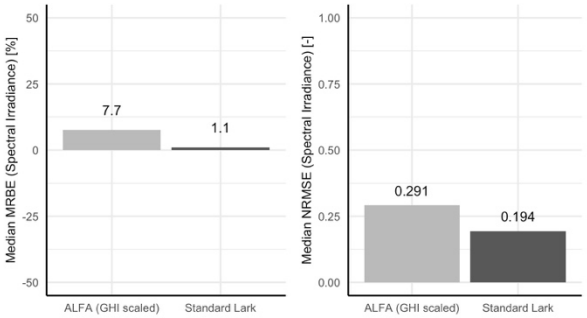

Figure 5: Median MRBE and NRMSE comparison between ALFA (GHI scaled) and standard Lark simulations.

The first element that was further studied was whether the actual measured sky SPD was necessary for accurate simulations of spectral irradiance in *Lark*, or if the SPD of the CIE Standard Illuminant D65 (D65) or of a theoretical flat spectrum (FS), i.e., with a constant value over the entire visible range, would be enough. Figure 6 shows the comparison of the simulation error between standard simulations in *Lark* using the measured SPD and simulations in *Lark* using the D65 or FS SPD.

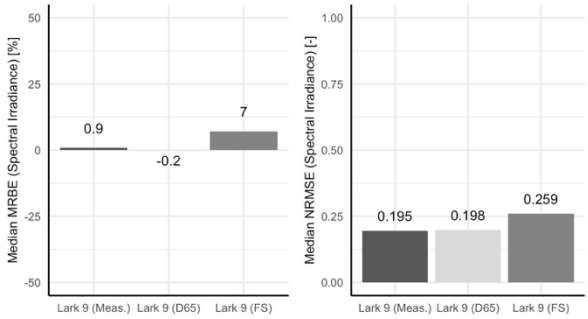

Figure 6: Median MRBE and NRMSE comparison between Lark simulations with measured, D65, and FS SPD.

It can be observed that, at least for middle latitudes, using the D65 SPD instead of a measured SPD does not impact the accuracy of the simulated spectral irradiance. However, a positive bias and higher fluctuation from the measurements can be observed when the FS SPD is used.

Another investigation focused on how much 9-channel simulations improved the accuracy of simulated spectral irradiance in comparison to 3-channel simulations. The spectra generated through standard *Lark* 9-channel simulations were analyzed against the spectra generated through *Lark* 3-channel simulations, and against spectra generated by scaling a D65 SPD with the photometric results of basic *Radiance* RGB simulations. To better understand the difference between these three types of simulated spectral irradiance, the three simulated spectra are provided in Figure 7 for a given moment and location together with the measured spectrum.

From the comparison of the simulation error between the three types of simulation (Figure 8), it can be observed that the most accurate simulation type is the *Lark* 9-channel simulation. However, *Radiance* RGB simulations whose outputs are used to scale a D65 SPD still produce relatively accurate spectral irradiance values compared to 9-channel simulations, though with a slight positive bias.

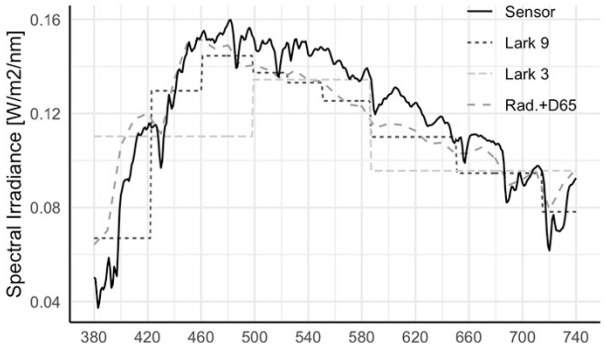

Figure 7: Measured and simulated spectral irradiance (intermediate sky in August, Lausanne, desk 1).

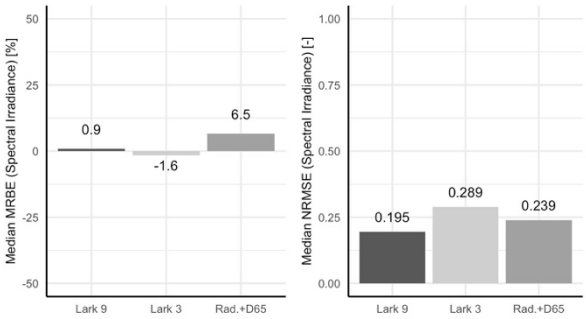

Figure 8: Median MRBE and NRMSE comparison between Lark simulations with 9 and 3 channels, and Radiance RGB simulations scaled with D65 SPD.

Finally, further insights were sought regarding the performance of the new gendaylit colored sky option (Wienold et al., 2018). The simulation errors of *Lark* 3-channel simulations using the measured sky SPDs, the D65 SPD, and the FS SPD were thus compared to the errors of *Radiance* RGB simulations with the basic gray and the colored gendaylit sky models (Figure 9).

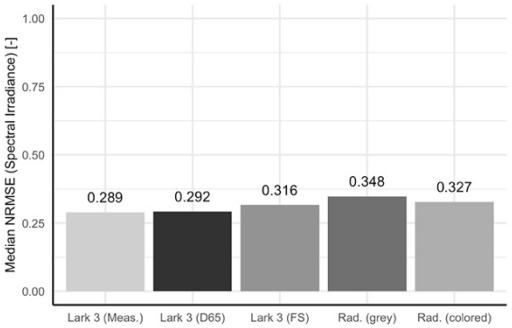

Figure 9: Median NRMSE comparison between Lark simulations with measured, D65, and FS SPD, and Radiance RGB simulations with gendaylit gray and colored sky models.

Although the difference between the five 3-channel simulation types is relatively weak, the *Lark* 3-channel simulations based on the measured and D65 SPD perform best. Compared to these two simulation types, the *Radiance* RGB simulations with the colored gendaylit sky model show a slightly higher median NRMSE. A further investigation by sky type demonstrated that the median

NRMSE of the simulations with the gendaylit colored sky option is surprisingly high under clear skies (Figure 10).

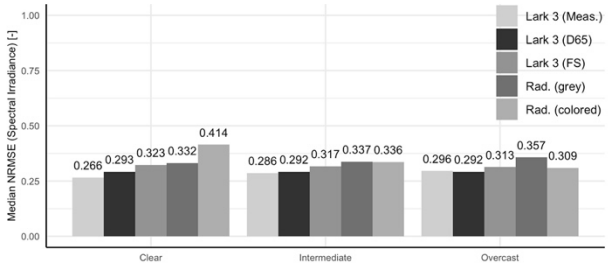

Figure 10: Median NRMSE comparison between Lark simulations with measured, D65, and FS SPD, and Radiance RGB simulations with gendaylit gray and colored sky model for the three different sky conditions.

By looking directly at the simulated spectra for a given moment and under a clear sky (Figure 11), it can be observed that the simulations relying on the gendaylit colored sky option overestimate the blue component of the sky for clear sky conditions.

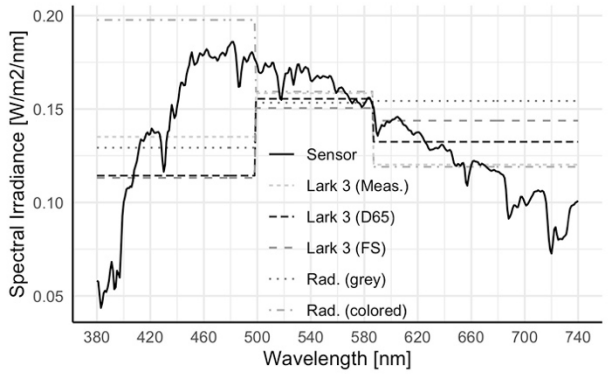

Figure 11: Measured and simulated spectral irradiance (clear sky in August, Lausanne, desk 1).

Of all the different types of simulations tested here, the *Lark* 9-channel simulations based on either a measured or the D65 SPD are those that present no bias and the lowest average NRMSE. The distributions of the MRBE of these simulations for each sky type (Figure 12) is in fact very similar to those of the RE in vertical illuminance of basic *Radiance* RGB simulations shown in Figure 2 and to what is found for *Radiance* simulation validation in the literature (Mardaljevic, 1999).

At last, the simulation time varies between the different types of spectral simulation applied here. In Figure 13, the time for one simulation run conducted on the same computer for different simulation types is analyzed in function of the accuracy of that simulation type described by its median and percentiles 25 and 75 NRMSE. It can be observed that the best performing simulation type, i.e., the *Lark* 9-channel simulation, is also the one taking the longest. Regarding *ALFA* simulations, increasing the number of passes extends the simulation time for only a small improvement in median NRMSE. A basic *Radiance* RGB simulation of which the output is used to scale a D65 SPD seems to be a good compromise to significantly shorten the simulation time while offering an acceptable accuracy in comparison to a *Lark* 9-channel simulation. However, 3-channel simulations (represented by empty triangles in Figure 13) might only offer such accuracy for indoor environments with relatively neutral colors like in this study, as the spectral information of the scene is averaged over 3 channels during the simulation.

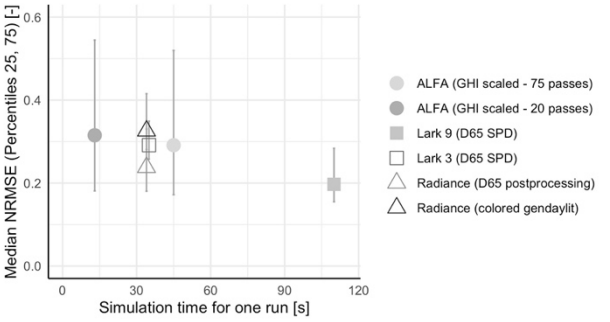

Figure 13: Median NRMSE versus simulation time; the symbol represents the simulation tool (ALFA, Lark, or Radiance) and an empty symbol is used when it is a 3-channel simulation type.

Conclusion

In this study, two spectral simulation tools developed for building simulation purposes (*ALFA* and *Lark*) were tested for their accuracy in predicting building occupants' daylight exposure in terms of spectral irradiance over time. The validation data contains spectral irradiance measured over several days at three desk positions in two office-like laboratory rooms in Eindhoven and Lausanne.

The results show that *Lark* 9-channel simulations, despite being the most time-consuming spectral simulation type, provide the most accurate results, with no bias and an error distribution similar to what can be expected from a standard *Radiance* RGB simulation, i.e., most errors within the ±20% range (Figure 12). Additionally, it has been demonstrated that for middle latitudes, a D65 SPD can be input in *Lark* instead of a measured sky SPD

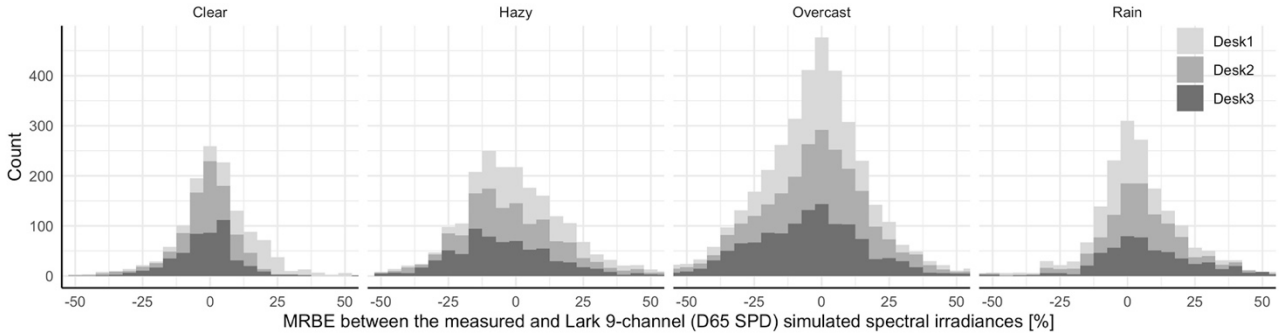

Figure 12: Distribution of MRBE between the measured and Lark 9-channel simulated spectral irradiance by sky condition for both locations and for each desk position.

without impacting the accuracy of the simulated spectral irradiance. However, it should be noted that the *Lark* tool is not as user-friendly as *ALFA*, as it requires some knowledge in *Radiance* (to correctly define the simulation parameters), in *Grasshopper* (to establish the simulation flow), and in *Python* coding (to modify the published *Lark* components when needed). Furthermore, *Lark* asks for additional inputs, such as the sky irradiance, which makes its results more accurate but its use less adapted to the design process. Finally, *Lark* considers a unique SPD over the entire sky dome, unlike *ALFA*, hence not accounting for changes in spectral characteristics with sky orientation (Diakite-Kortlever & Knoop, 2021). In that regard, the new gendaylit colored sky option was tested against different types of 3-channel simulation, as it applies an empirically verified relation between the CCT and the luminance of the sky to color the sky dome. Although promising, the colored sky option in gendaylit seems to overestimate the blue component of the sky for clear sky conditions, hence requiring some future adjustments.

Since the intended use of these spectral simulation tools is the study of non-visual responses to light, it would be pertinent to determine the extent to which such simulation errors may actually affect the output of non-visual response models. This will be studied in a future publication, which will open the discussion about the significance of a difference in light exposure when it comes to non-visual responses. Indeed, only when non-visual responses to light are better understood, will we be able to evaluate whether a difference in exposure matters, and thereby have the means to determine relevant error thresholds for spectral simulation tools.

Acknowledgement

This project has received funding from the European Union's Horizon 2020 research and innovation programme under the Marie Skłodowska-Curie grant agreement No 754462.

References

Acosta, I., Leslie, R., & Figueiro, M. (2017). Analysis of circadian stimulus allowed by daylighting in hospital rooms. *Lighting Research & Technology*, *49*(1), 49–61.

Altenberg Vaz, N., & Inanici, M. (2020). Syncing with the Sky: Daylight-Driven Circadian Lighting Design. *LEUKOS*.

Amirazar, A., Azarbayjani, M., et al. (2018). *Assessing the Circadian Potential of an Office Building in the Southeastern US*. SimAUD 2018, Delft, The Netherlands.

Amundadottir, M. L., Rockcastle, S., Sarey Khanie, M., & Andersen, M. (2017). A human-centric approach to assess daylight in buildings for non-visual health potential, visual interest and gaze behavior. *Building and Environment*, *113*, 5–21.

Amundadottir, M., Lockley, S., & Andersen, M. (2013). *Simulation-based evaluation of non-visual responses to daylight: Proof-of-concept study of healthcare re-design*. BS2013, Chambéry, France.

Andersen, M., Mardaljevic, J., & Lockley, S. (2011). A framework for predicting the non-visual effects of daylight - 1: Photobiology-based model. *Lighting Research & Technology*, *44*(1), 37–53.

Ayoub, M. (2020). A review on light transport algorithms and simulation tools to model daylight inside buildings. *Solar Energy*, *198, 623-642*.

Badosa, J., Wood, J., Blanc, P., Long, C. N., Vuilleumier, L., Demengel, D., & Haeffelin, M. (2014). Solar irradiances measured using SPN1 radiometers: Uncertainties and clues for development. *Atmospheric Measurement Techniques*, *7*(12), 4267–4283.

Balakrishnan, P., & Jakubiec, J. A. (2019). *Spectral Rendering with Daylight: A Comparison of Two Spectral Daylight Simulation Platforms*. BS2019, Rome, Italy.

Borisuit, A., Kämpf, J., Münch, M., Thanachareonkit, A., & Scartezzini, J.-L. (2016). Monitoring and rendering of visual and photo-biological properties of daylight-redirecting systems. *Solar Energy*, *129*, 297–9.

Brainard, G. C., Hanifin, J. P., Greeson, J. M., Byrne, B., Glickman, G., Gerner, E., & Rollag, M. D. (2001). Action Spectrum for Melatonin Regulation in Humans: Evidence for a Novel Circadian Photoreceptor. *Journal of Neuroscience*, *21*(16), 6405–6412.

CIE. (2018). *International Standard: CIE System for Metrology of Optical Radiation for ipRGC-Influenced Responses to Light* (CIE S 026/E:2018). Commission Internationale de l'Eclairage.

Delahunt, P., & Brainard, D. (2004). Does human color constancy incorporate the statistical regularity of daylight? *Journal of Vision*, *4*.

Diakite-Kortlever, A., & Knoop, M. (2021). Forecast accuracy of existing luminance-related spectral sky models and their practical implications for the assessment of the non-image-forming effectiveness of daylight. *Lighting Research & Technology*.

Geisler-Moroder, D., & Dür, A. (2010). *Estimating Melatonin Suppression and Photosynthesis Activity in Real-World Scenes from Computer Generated Images*. CGIV/MCS, Joensuu, Finland.

Gul, M. S., Kotak, Y. S., Muneer, T., & Ivanova, S. (2018). Enhancement of Albedo for Solar Energy Gain with Particular Emphasis on Overcast Skies. *Energies*, *11*(11), 2881.

Helliwell, R. (2012). Site layout planning for daylight and sunlight: a guide to good practice. *Arboricultural Journal*, *34*(1), 52–54.

Inanici, M., Brennan, M., & Clark, E. (2015). *Spectral Daylighting Simulations: Computing Circadian Light*. BS2015, Hyderabad, India.

Inanici, M., & ZGF Architects LLP. (2015). *Lark Spectral Lighting*.

Konis, K. (2016). A novel circadian daylight metric for building design and evaluation. *Building and Environment*, *113*, 22–38.

Kruisselbrink, T., Aries, M. B. C., & Rosemann, A. (2017). A practical device for measuring the luminance distribution. *International Journal of Sustainable Lighting*, *36*, 75–90.

LBNL. (2013). *Optics Version 6.0*.

Lucas, R. J., Peirson, S. N., et al. (2014). Measuring and using light in the melanopsin age. *Trends in Neurosciences*, *37*(1), 1–9.

Mardaljevic, J. (1999). *Daylight Simulation: Validation, Sky Models and Daylight Coefficients* [PhD dissertation]. De Montfort University.

McNeel, R., Gillespie, B., & Associates. (2020). *Rhinoceros version 6.0*.

Ochoa, C. E., Aries, M. B. C., & Hensen, J. L. M. (2012). State of the art in lighting simulation for building science: A literature review. *Journal of Building Performance Simulation*, *5*(4), 209–233.

OpenStreetMap contributors. (2017). *OpenStreetMap*.

Pechacek, C. S., Andersen, M., & Lockley, S. W. (2008). Preliminary method for prospective analysis of the circadian efficacy of (day)light with applications to healthcare architecture. *LEUKOS*, *5*(1), 1–26.

Perez, R., Ineichen, P., Seals, R., Michalsky, J., & Stewart, R. (1990). Modeling daylight availability and irradiance components from direct and global irradiance. *Solar Energy*, *44*(5), 271–289.

Potočnik, J., & Košir, M. (2021). Influence of geometrical and optical building parameters on the circadian daylighting of an office. *Journal of Building Engineering*, *42*, 102402.

Reinhart, C., & Andersen, M. (2006). Development and validation of a Radiance model for a translucent panel. *Energy and Buildings*, *38*(7).

Ruppertsberg, & Bloj. (2006). Rendering complex scenes for psychophysics using Radiance: How accurate can you get? *JOSA A*, *23*(4), 759–768.

Ruppertsberg, & Bloj. (2008). Creating physically accurate visual stimuli for free: Spectral rendering with Radiance. *Behavior Research Methods*, *40*(1), 304–308.

Solemma&Alertness CRC (2018). *Adaptive lighting for alertness ALFA*.

Tregenza, P., Stewart, L., & Sharples, S. (1999). Reduction of glazing transmittance by atmospheric pollutants. *Lighting Research & Technology*, *31*, 135–138.

Wandachowicz, K. (2006). *Calculation of Circadian Illuminance Distribution with Radiance*. Intl. Radiance Workshop, Leicester, UK.

Ward, G. (1987). *Radiance*. https://radiance-online.org//

Wienold, J., Diakite, A., Knoop, M., & Andersen, M. (2018). *Making simulations more colorful: Extension of gendaylit to create a colored sky*. Intl. Radiance Workshop, Loughborough, UK.

Xiao, H., Cai, H., & Li, X. (2021). Non-visual effects of indoor light environment on humans: A review. Physiology & Behavior, 228.

Yang, J. N., & Maloney, L. T. (2001). Illuminant cues in surface color perception: Tests of three candidate cues. Vision Research, 41(20).